Liquid Crystals
Publication details, including instructions for authors and subscription information:
http://www.informaworld.com/smpp/title~content=t713926090

Small angle X-ray scattering study of chiral side chain liquid crystalline polymers in 5CB and 8CB solvents

Fabiano V. Pereira[a][b]; Redouane Borsali[b]; Aloir A. Merlo[a]; Nadya P. Da Silveira Corresponding author[a]
[a] LCPO-CNRS-ENSCPB Bordeaux University (UMR5629), 33607 Pessac, France [b] Instituto de Química, Universidade Federal do Rio Grande do Sul, CEP 91501-970 Porto Alegre-RS, Brazil

To cite this Article Pereira, Fabiano V. , Borsali, Redouane , Merlo, Aloir A. and Da Silveira Corresponding author, Nadya P.(2004) 'Small angle X-ray scattering study of chiral side chain liquid crystalline polymers in 5CB and 8CB solvents', Liquid Crystals, 31: 5, 655 — 661

To link to this Article: DOI: 10.1080/02678290410001668019

URL: http://dx.doi.org/10.1080/02678290410001668019

LIQUID CRYSTALS, VOL. 31, NO. 5, MAY 2004, 655–661

Small angle X-ray scattering study of chiral side chain liquid crystalline polymers in 5CB and 8CB solvents

FABIANO V. PEREIRA[†‡], REDOUANE BORSALI[‡], ALOIR A. MERLO[†]
and NADYA P. DA SILVEIRA[*†]

[†]LCPO-CNRS-ENSCPB Bordeaux University (UMR5629),
16 Avenue Pey Berland, 33607 Pessac, France
[‡]Instituto de Química, Universidade Federal do Rio Grande do Sul,
Av. Bento Gonçalves 9500, CEP 91501-970 Porto Alegre-RS, Brazil

(*Received 10 October 2003; in final form 21 December 2003; accepted 31 December 2003*)

Small angle X-ray scattering was used to examine the new chiral side chain liquid crystalline polyacrylates (P_{4M} and P_{11M}) and their mixtures (2 wt %) in the low molar mass nematogenics 4′-*n*-pentyl-4-cyanobiphenyl (5CB) and 4′-octyl-4-cyanobiphenyl (8CB). Complementary data were obtained by polarizing optical microscopy. In agreement with previous studies, the mesophases of the bulk polymers show a dependence on the aliphatic spacers linking the mesogenic units to the polymer backbone. Chiral nematic and smectic A_1 phases were observed for the polyacrylates with four (P_{4M}) and eleven (P_{11M}) methylene units as spacers, respectively. In solution with 5CB and 8CB, P_{4M} exhibits an injected smectic phase, whereas P_{11M} maintains the smectic arrangement already observed in the bulk, with swollen smectic layers. In all the mixtures, layer stability was found to depend on the liquid crystal used as solvent, as well as on the temperature. At temperatures corresponding to the nematic 5CB and 8CB, the coexistence of two mesophases was observed in the mixtures. Moreover, with the liquid crystal solvents in the isotropic phase, microstructures suspended in the solvent matrix containing the liquid crystalline polymer in the smectic arrangement were detected.

1. Introduction

Mixtures consisting of polymers and low molar mass nematogenics (LMMNs) represent an interesting class of materials due to their physical and chemical properties. Apart from the fundamental interest, the order range in this kind of mixture constitutes a problem in the technological display industry, where layer alignment by polymer confinement is the key to success of any liquid crystal display panel [1].

In pursuit of novel liquid crystal phase behaviour and properties, many polymer/LMMN composites have already been developed as thin films [2]. These can be divided into different categories such as polymer dispersed liquid crystals (PDLCs) and polymer stabilized liquid crystals (PSLCs) [3, 4]. Usually, a PDLC can be prepared by encapsulation, starting from an emulsion of liquid crystal droplets in polymer solution, or by phase separation. On the other hand, a PSLC can be obtained from a simple mixture of the polymer in an LMMN or by dissolving a small amount of the monomer in an LMMN followed by thermal or photoinduced polymerization producing a polymer network [5]. Theoretical and experimental studies on PSLCs have been performed in recent years mostly exploring the different phases in the systems as a function of polymer concentration by phase diagrams [1, 6–11].

In a PSLC, it is known that polymer chains tend to form a network that aligns the liquid crystal [12]. There is also a tendency of the chain to be aligned with the anisotropic field of the LMMN, defining an anisotropic shape for the polymer [13]. The degree of anisotropy depends on the flexibility of the polymer backbone, molecular mass, spacer length and whether the polymer exhibits nematic or smectic phases. For the mixtures containing a liquid crystalline polymer, the average nematic axis is defined by the director **n** of the LMMN and, although the polymer chains exhibit a distribution of orientations, the mesogenic groups in the polymer tend to orient parallel to the vector director of the liquid crystal solvent [13].

Liquid crystalline polymers with lateral mesogenic groups possess considerable application potential in the design of optical and electro-optical devices [2].

---

[*]Author for correspondence; e-mail: nadya@iq.ufrgs.br

Liquid Crystals ISSN 0267-8292 print/ISSN 1366-5855 online © 2004 Taylor & Francis Ltd
http://www.tandf.co.uk/journals
DOI: 10.1080/02678290410001668019

Recently, we have described the synthesis and structure–property correlations for a series of new different thermotropic side chain liquid crystalline polymers (SCLCPs) containing different mesogenic side groups [14–17]. Searching for new systems containing SCLCPs, we focus in the present study on the behaviour of these SCLCPs in the presence of liquid crystal solvents.

In this context, we have investigated the molecular organization of mixtures formed by two chiral SCLCPs, P_{11M} and P_{4M}, in two LMMNs, 4′-*n*-pentyl-4-cyanobiphenyl (5CB) and 4′-octyl-4-cyanobiphenyl (8CB), by means of small angle X-ray scattering (SAXS). The polymer P_{11M} contains eleven methylene units as spacer and presents a chiral smectic A phase (Sm*A), whereas P_{4M} has four methylene units as spacer and presents a nematic chiral (N*), known as a cholesteric phase. At room temperature, 5CB and 8CB are nematic and smectic solvents, respectively. Their chemical structures are illustrated in figure 1. In order to analyse and illustrate the phase behaviour of the samples, we also employed polarizing optical microscopy (POM).

Finally, since we are not using thin films, this work represents a first step towards the possibilities of applying this kind of system to control or promote liquid crystalline orientation in low concentration SCLCP solutions, with the polymer network offering bulk effects. These properties might be of advantage, for example, in the alignment and/or stabilization of liquid crystalline materials in relatively thick films for technological applications.

2. Experimental section

The chiral SCLCPs were synthesized using direct radical polymerization of a mesogenic acrylate monomer. Details of the synthesis are described elsewhere [14–16]. The LMMNs, 5CB and 8CB, were purchased from Aldrich Chemicals and used as received. The mesomorphic properties of the SCLCPs and LMMNs were determined from POM, differential scanning calorimetry (DSC) and SAXS. The molar masses and transition temperatures of the polyacrylates P_{4M} and P_{11M}, as well as of the liquid crystalline solvents 5CB and 8CB, are listed in table 1.

Table 1. Molecular weights ($g\,mol^{-1}$) and transition temperatures (°C) of the polymers and low molar mass nematogenics. Gr = glassy state, Sm = smectic phase, N = nematic phase, I = isotropic phase. For the polymers, M_n was determined from size exclusion chromatography and transition temperatures were obtained from DSC measurements. Data for 5CB and 8CB were taken from the literature.

Material	M_n	Gr		Sm		N		I
P_{4M}	10 570	●	43.8			●	81.2	●
P_{11M}	25 780	●	60.7	●	110.3			●
5CB	236		21.5			●	35.0	●
8CB	278		22.5	●	33.3	●	39.8	●

In order to prepare the samples, a known amount of each SCLCP was mixed with the corresponding LMMN. The samples were heated 30°C above the LMMN clearing temperature and ultrasonicated for at least 12 h to make a homogeneous mixture. The treatment with ultrasound produced a homogeneous mixture on a macroscopic scale with up to about 5 wt% of polymer. It was not possible to prepare the mixtures above the $T_{Sm\text{-}I}$ of the polymers due to the flash point of the LMMNs.

For polymer concentrations below 2 wt%, a low

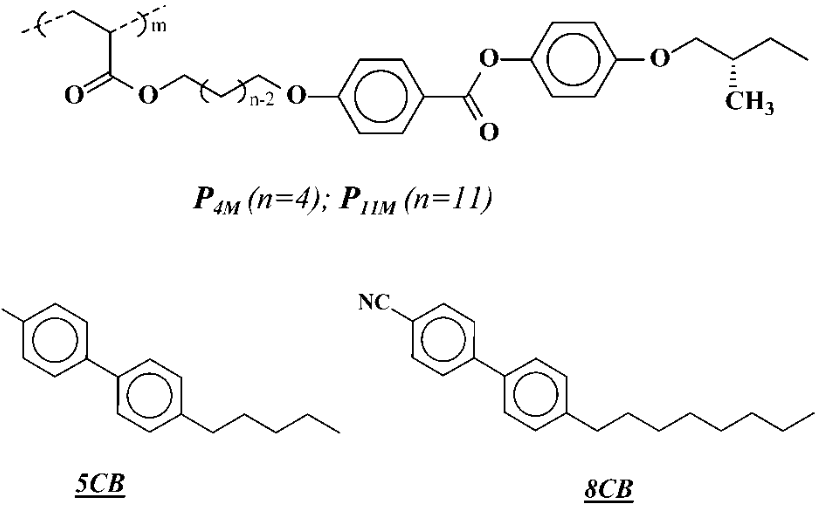

Figure 1. General chemical structures of the chiral liquid crystal polyacrylates P_{4M} and P_{11M} and the low molar mass nematogenics 5CB and 8CB.

signal-to-noise ratio in the X-ray spectra was detected. Thus, we performed most of the SAXS measurements with samples containing 2 wt% of SCLCP, and all results presented here are from 2 wt% mixtures. It is important to mention here that no concentration dependence of the X-ray spectra in the concentration range from 0.5 to 5 wt% was observed.

The samples were placed in quartz capillaries of 1.5 mm diameter. Most of the SAXS measurements were carried out using a computer-controlled Nanostar X-ray system (LCPO, Bordeaux, France). Additional results were obtained on the bending magnetic beamline BM2 at the European Synchrotron Radiation Facility (ESRF, Grenoble, France) and on the Laboratório Nacional de Luz Síncrotron (LNLS, Campinas, Brazil). In the Nanostar equipment, the X-rays were generated from a rotating anode producing Cu K_α radiation with the wavelength $\lambda = 1.54$ Å. A collimated beam was passed horizontally through an evacuated chamber containing the sample and diffracted on a 2D detector. The sample was suspended vertically in a hot stage having an accuracy of ± 0.1°C. An exposure time of about 18 h was required for all the samples. At ESRF, λ was 0.775 Å and an indirect illumination CCD detector (Princeton Instruments) was used at 55.0 cm from the sample. The exposure times were about 50 s in this case. Silver behenate was used for calibration in both SAXS set-ups. At LNLS, λ was 1.608 Å and a linear detector was employed.

Attempts to determine the mesophase behaviour of the mixtures by means of DSC failed due to the low polymer content. In these mixtures, DSC thermograms display only peaks associated with the LMMN transitions. The mesomorphic behaviour of the mixtures (2 wt%) was therefore followed by analysis of the textures as a function of temperature using an Olympus BX41 optical polarizing microscope coupled to a Quasar MT300 hot stage.

3. Results and discussion

3.1. *The bulk samples*

Figure 2 shows the SAXS profiles obtained with P_{4M}, P_{11M}, 5CB and 8CB in their characteristic mesophases. The values of *d*, extracted from the SAXS profiles, are given in table 2. They were determined by the relation $2\pi/q$, with *q* representing the wave vector. In a nematic phase, *d* roughly corresponds to the length of the interdigitated structure, whereas in a smectic phase, it corresponds to the length of the smectic layers. In table 2 we also list the values of *L* and *d*/*L*. In this work, *L* is the theoretical length of the mesogenic moieties including, in the case of the polymers, the spacers, and represents a good estimate for the molecular size of the LMMNs. *L* was obtained from geometry optimization using the MNDO-PM3 [18] semiempirical parametrization for distance calculations, followed by GEPOL calculations [19, 20]. The ratio *d*/*L* was also used to elucidate the mesophase arrangement of the polymers in the bulk and in the mixtures.

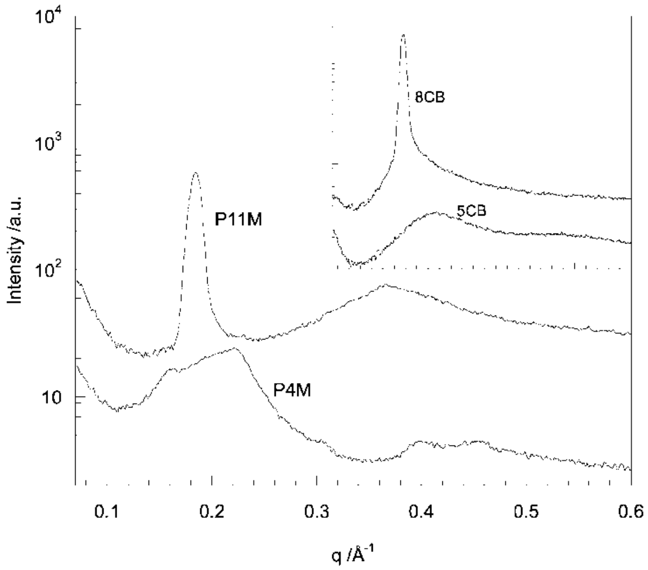

Figure 2. Small angle X-ray scattering profiles of the chiral liquid crystal polyacrylates P_{4M} (50°C) and P_{11M} (70°C) and the low molar mass nematogenics 5CB and 8CB (room temperature).

The X-ray 2D diffraction image of the polymer P_{4M} (not shown here) presents a diffuse scattering ring characteristic for a nematic phase. This reflects a weak positional short-range order with a preferential direction of the mesogenic groups, known as orientational order. Due to the small flexible spacer, this polymer does not allow decoupling between the mesogenic group and the backbone and, as a consequence, positional correlations in the nematic phase are weak, only extending over short distances. The SAXS profile of P_{4M} in figure 2 exhibits the broad feature typical for a nematic phase. This maximum at $q \approx 0.185$ Å^{-1}

Table 2. Layer spacing *d*(Å) at room temperature, theoretical length of mesogenic groups *L*(Å), and *d*/*L* ratios.

Material	*d*	*L*	*d*/*L*
P_{4M}	34.0 ± 6.0	30.2	—
P_{11M}	35.4	35.4	1.0
5CB	24.8 ± 7.0	16.2	—
8CB	31.1	19.8	1.6
P_{11M}/5CB	60.9	35.4[a]	1.7
P_{11M}/8CB	66.1	35.4[a]	1.9
P_{4M}/5CB	47.2	30.2[a]	1.6
P_{4M}/8CB	49.6	30.2[a]	1.6

[a] Values for the mesogenic in the polymer.

corresponds roughly to the length *d* from repeated polymer units. The experimental value of *d* determined from SAXS for P_{4M} is very close to the theoretical value *L* (table 2). The nematic phase can be observed in P_{4M} from 43.8 to 81.2°C, as determined by DSC measurements. At room temperature, the scattering profile of this polymer is very similar to that shown in figure 2 because the molecular orientational order depends only slightly on temperature. In fact, the principal difference between the crystalline and nematic phases in this type of system are molecular motions in the fluid-ordered mesophase that can be studied by wide angle X-ray scattering (WAXS) [21]. In the *q* range covered by WAXS, the diffuse ring due to intermolecular interference perpendicular to the director can be detected and related to the distance between two lateral mesogenic groups of the same backbone. This ring is sharper in a crystalline phase than in a liquid crystalline mesophase.

Figure 2 also shows the smectic layered phase of P_{11M} at 70°C. The mesogenic lateral groups are the same as in P_{4M}. However, the mesomorphic behaviour of P_{11M} is quite different due to the extension of the flexible spacer. The mesogenic moieties are considerably decoupled from the backbone and, consequently, the polymer presents a positional order in addition to the orientational order. The subsequent packing of the backbone ribbons creates layers resulting in the smectic mesophase. The X-ray 2D diffraction image of P_{11M} (not shown here) consists of two rings ($q=0.177$ and $0.355\,\text{Å}^{-1}$) with nearly uniform intensities, indicating smectic layers without preferred directions. Similar to P_{4M}, the scattering profile of P_{11M} at room temperature is the same as at 70°C, as depicted in figure 2. Thus, no changes in the packing arrangement of the backbone were found in this temperature range. The first sharp peak in the P_{11M} profile defines the *d* spacing between the smectic layers. The reflection at $q=0.355\,\text{Å}^{-1}$ is diffuse and can be attributed to the underlying polymer backbone [21]. For polymeric smectic phases, it is known that the main chains are kept preferentially between the layers if the spacers are flexible, resulting in an SAXS diffuse ring [16]. Otherwise, measurements performed at the ESRF using higher X-ray intensity, with the polymer in the smectic mesophase, indicated the presence of a sharp second-order peak at the same *q* value as the diffuse ring. The relation between the first and second Bragg peaks was determined as 1:2. As the values of *d* and *L* agree very well for P_{11M} (table 2), the ratio $d/L=1$ characterizes a large overlap of mesogenic units, with the smectic structure presenting monolayer character, i.e. Sm^*A_1 [21]. In addition, the polymer was oriented in a magnetic field (12 T), and the resulting X-ray 2D image presented characteristics of the SmA mesophase, possessing two spots with a lamellar relation (1:2 ratio) between them.

The diffraction image (not shown here) of the nematic mesophase in 5CB contains spots, indicating a preferential direction. The alignment of the sample under the action of the capillary tube is facilitated due to the low viscosity of 5CB. The SAXS profile of 5CB in figure 2 shows a large peak located at $q=0.254\,\text{Å}^{-1}$ ($d=24.75\,\text{Å}$) corresponding almost to the length of the interdigitated 5CB geometry. The sharp peak of the smectic phase in 8CB can also be seen in figure 2. In this case, the value of *d* corresponds to the layer size (31.10 Å). The ratio $d/L=1.57$ suggests a partially interdigitated smectic A phase, easily explained by the chemical structure of 8CB depicted in figure 1. No preferential direction was observed in the SAXS diffraction image of 8CB, in contrast to 5CB. At room temperature, the larger viscosity of 8CB over 5CB makes the alignment of the sample difficult.

3.2. *The mixtures*

In figures 3 (*a*) and 3 (*b*), we depict the SAXS profiles for the mixtures P_{11M}/5CB and P_{11M}/8CB, respectively. One sharp peak, together with a broad feature, can be seen for the bulk P_{11M} in figure 2, whereas three peaks can be observed for the mixtures in figure 3. The top curve in 3(*b*) corresponds to a spectrum obtained at the ESRF, where the first peak can be better observed. The first peak corresponds to the size of the layered structure *d* in each case, listed in table 2. The ratio between the reflections (1:2:3) in the mixtures indicates the presence of a lamellar structure. Furthermore, sharp peaks can be observed for the solutions, differently from bulk P_{11M}. These peaks appear to be due to the influence of the anisotropic field of the solvent, which affects the internal molecular degrees of freedom in the polymer. Simultaneously, the low molar mass nematogenic induces lateral orientation of the mesogenic groups in the polymer and contributes to the stiffness of the backbone, which seems to be more important than in the bulk. The second and more intense peak in the P_{11M}/8CB curves corresponds principally to reflection from the 8CB, hiding an expected second Bragg reflection from the smectic layers.

The X-ray 2D images obtained for mixtures with 5CB indicated a preferential orientation of the polymer chains with respect to the solvent, as depicted in the inset in figure 3 (*a*). The low viscosity facilitates the alignment. This result suggests an anchoring effect of the solvent, indicating that the origin of the preferential direction in the SCLCP orientation is due to the anisotropic field of the nematic solvent. This suggests that the preferential orientation of the cyanobiphenyl

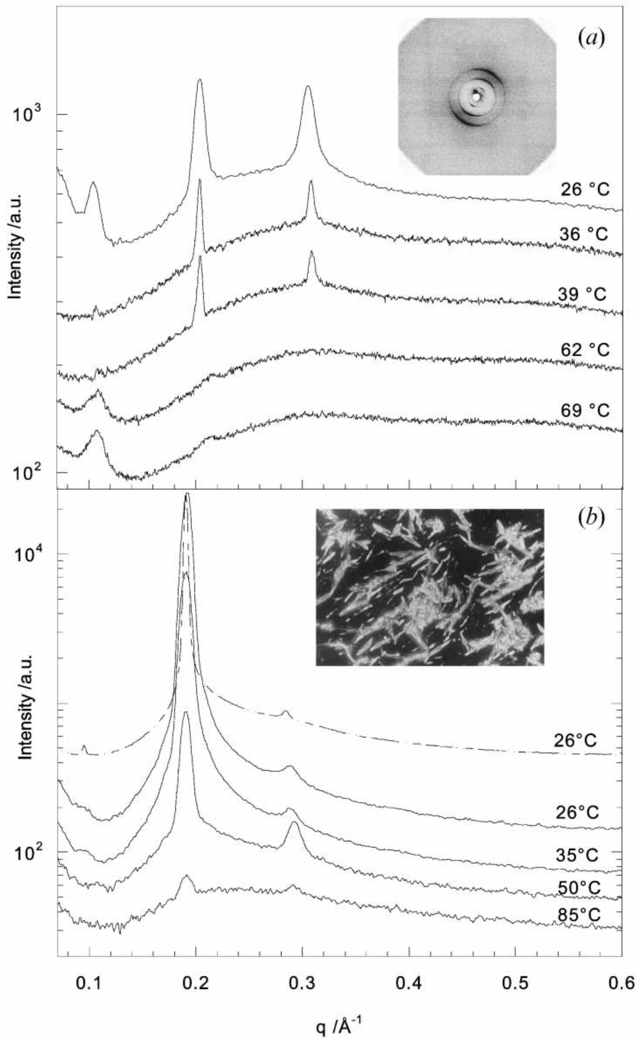

Figure 3. Small angle X-ray scattering profiles of P_{11M} in (*a*) 5CB and (*b*) 8CB as a function of temperature in a heating cycle. The top curve in (b) corresponds to a spectrum obtained at the ESRF. The inset in (a) shows an X-ray 2D image for the mixture at 26°C and the inset in (*b*) gives a micrograph (40 ×) of the mixture containing the polymer in the smectic phase (*bâttonets*, at 55°C), suspended in the isotropic matrix of 8CB.

moieties is parallel to the lateral mesogenic groups of the polymer and, consequently, the director of the solvent is perpendicular to the backbone.

The layer sizes *d* obtained by analysis of the first Bragg peak in the mixtures are also given in table 2. Larger smectic layers than in bulk P_{11M} were observed for P_{11M}/5CB and P_{11M}/8CB. They are the consequence of a swelling effect produced by the solvent occupying preferentially spaces in the layers. The effect is more pronounced for the solution containing 8CB, due to the length of the terminal alkyl tail (see figure 1). Consequently, the interdigitation degree in the system P_{11M}/5CB is more important than in the mixtures containing P_{11M}/8CB. Additionally, these results suggest that the lateral mesogenic groups attached to the polymer are oriented in relation to the solvent moieties, with a consequent backbone packing perpendicular to the solvent director. Therefore the molecular size and nature of the solvent play an important role in the packing order and also determine distances between the backbone ribbons. It becomes, in fact, a way to control the interlayer distances in an SCLCP.

For the bulk P_{4M}, the rigidity of the spacers hinders positional order. Therefore only a nematic phase is observed, which is responsible for the broad feature shown in figure 2. The SAXS profiles for mixtures of P_{4M} in 5CB and 8CB are presented in figures 4 (*a*) and 4 (*b*), respectively. Peaks with a ratio characteristic of lamellar structures (1:2:3) can be observed in both cases, independently of the solvent used. An induced smectic phase from the mixture of two nematic materials has been described in the literature as a consequence of strong mesogenic interactions [12]. Indeed, a theoretical model has been developed in order to explain this phenomenon by combining Flory–Huggins (FH) [22] theory for isotropic mixing and Maier–Saupe–McMillan (MSM) [23] theory for smectic ordering in the nematic mixture.

As expected, *d* values obtained from the first Bragg peaks are larger for the solution containing 8CB than those obtained with 5CB, due to the different sizes of the LMMNs. From the broad pattern underlying the second Bragg peak in the SAXS profiles of P_{4M}/5CB, the coexistence of a nematic arrangement with the layered structures is suggested. The nematic texture obtained by means of POM corroborates this finding. A nematic texture was also observed for the sample containing P_{4M} in 8CB. However, due to the low polymer content in the mixtures, it was not possible to detect a smectic texture, as indicated in the SAXS profiles, by means of POM.

In contrast to the nematic phase in bulk P_{4M}, the origin of the smectic phase in P_{4M} solutions is related to LMMN interactions with the mesogenic unit in the polymer. If a lateral mesogenic group in an SCLCP is sufficiently decoupled from the polymer backbone, a smectic phase can be developed. According to our results, the LMMN induces the same effect as larger spacers between the mesogenic moiety and the polymer chain in P_{4M}. In this case, a relative decoupling of the lateral groups from the polymer backbone is possible due to their increasing mobility on addition of the anisotropic solvent. Consequently, a positional order among the lateral mesogenic groups and the packing of the backbone ribbons is achieved: the smectic phase. This solvent-induced ordering phenomenon is not possible in an ordinary isotropic solvent. We have also performed experiments using an organic solvent (tetrahydrofuran); in this case the liquid crystal order is lost even at high polymer concentrations (around 50 wt %).

The results of this work, such as the enhanced order in P_{4M} or the swelling effect in P_{11M}, demonstrate that local interactions as well as the architecture of the polymers play an important role in mesophase formation. We have prepared mixtures with another smectic polymer, containing a small spacer (four methylene units) and a large tail (ten methylene units), in the 8CB solvent. In this case, no swelling effect was observed in the polymer. Thus, the large tail formed by alkyl groups at the end of the mesogenic moiety interferes with the ingress of solvent between the layers. This mixture will be the subject of a future publication.

Temperature dependence represents an important tool for investigating the development of order as well as to understand better the interactions between the solvent and the polymer in this type of mixture. We have performed experiments in a temperature range covering the mesomorphic behaviour of the bulk solvents for all the samples studied. Figure 3 (*a*) shows the temperature dependence for the P_{11M}/5CB mixture. No temperature dependence can be observed in the position of the peaks, indicating that the packing of the backbones is similar within the investigated range of temperature, from room up to the isotropic phase. However, there is a temperature dependence in the intensity of the peaks. Considering the first peak at 36°C (with the solvent in the isotropic state) and above, the intensity is lower than at 26°C due to a smaller number of organized structures in solution. On increasing the temperature, the polymer chains become increasingly more flexible as a consequence of the increasing mobility of the attached mesogenic groups. Finally, at 69°C, the backbone motion drastically reduces the number of ordered regions, destroying the smectic structure in the mixture. Hence, a broad background can be seen between 0.2 and 0.4 Å^{-1} in figure 3(*a*) up to 69°C. This is related to a nematic phase coexisting with the lamellar smectic phase.

Figure 3 (*b*) shows the temperature effect for the sample containing P_{11M}/8CB. Smectic layers are present over a wide temperature range. By means of POM a focal-conic texture of the smectic phase was observed up to 35°C. For higher temperatures, where the solvent becomes isotropic, *bâtonnets* can be seen, as depicted in the inset in figure 3 (*b*) (55°C during heating), with the black regions corresponding to the solvent in the isotropic phase. The same behaviour was observed in the P_{11M}/5CB mixture using microscopy, at temperatures where the solvent is isotropic. Since a smectic phase can be seen in the P_{11M}/8CB mixture up to 85°C the arrangement between P_{11M} and 8CB is more stable than when 5CB is used as solvent.

The temperature dependence of the P_{4M}/5CB solution is depicted in figure 4 (*a*). The system exhibits smectic layers up to 65°C, when the layers begin to disappear due to thermal motions. Again, the system exhibits lamellar structure at a temperature above the clearing point of the solvent, indicating the existence of a stable phase. The inset in figure 4 (*a*) shows microstructures suspended in the isotropic matrix of the solvent, as obtained by POM at 39°C (during heating).

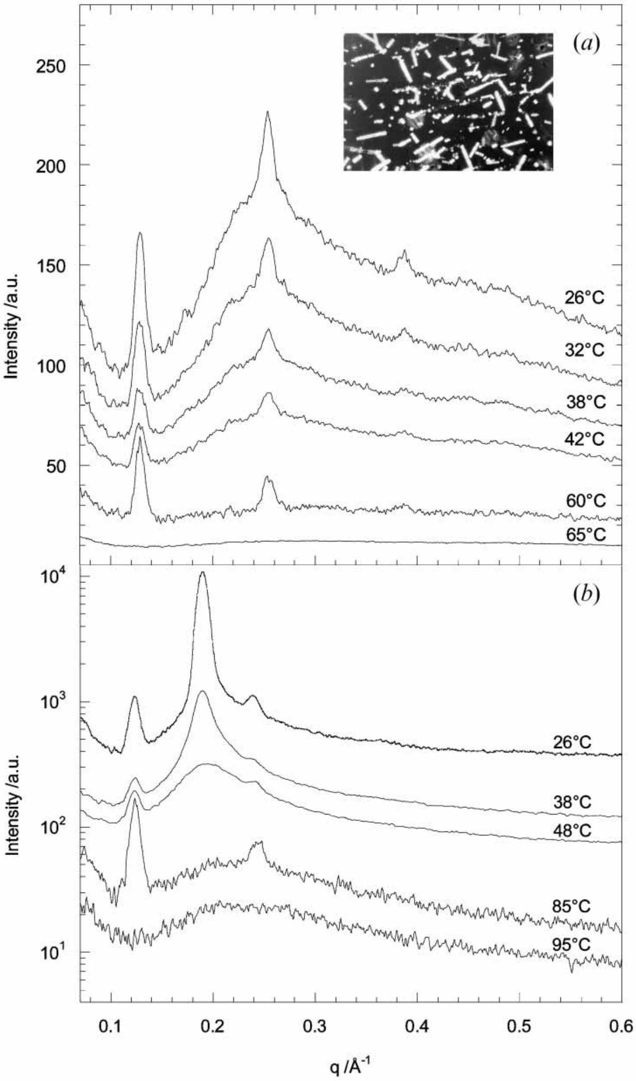

Figure 4. Small angle X-ray scattering profiles of P_{4M} in (*a*) 5CB and (*b*) 8CB as a function of temperature in a heating cycle. The inset shows a micrograph (10 ×) of the mixture containing the polymer in the smectic phase (*bâttonets*, at 39°C), suspended in the isotropic matrix of 5CB.

For the P_{4M}/8CB mixture, in figure 4 (*b*), the temperature dependence of the lamellar structures is similar to that observed in 5CB. However, in this case the system does not become isotropic until it reaches 95°C. Again, the arrangement induced by the 8CB solvent is more stable than when 5CB is used. Very similar results have been observed for the mixture containing P_{11M}. With eight carbon atoms in the terminal tail, 8CB allows more flexibility in the side mesogenic units attached to the polymer chain and stabilizes the layers in the mixture over a more extended temperature range than does 5CB.

4. Conclusions

Mesophases in bulk polymers show a dependence on the length of aliphatic spacers linking the mesogenic units to the backbone. A chiral nematic phase is observed for the polyacrylate with four methylene units whereas for the polymer with 11 methylene units as spacer a chiral smectic phase is observed.

We have modified the backbone conformation of both polymers using, as solvent, liquid crystals 5CB and 8CB. The nematic polymer P_{4M} develops an injected smectic A phase in the presence of the low molar mass nematogenics through a solvent-induced ordering phenomenon. The smectic polymer P_{11M} maintains the smectic phase observed in the bulk also in mixtures with 5CB and 8CB, with the appearance of swollen layers. The resulting smectic layers were determined by SAXS.

Layer stability in the mixtures seems to depend on the liquid crystal used as solvent. With eight carbon atoms in the terminal tail, 8CB gives more flexibility to the side mesogenic units attached to the polymer chain, stabilizing the layers over an extended temperature range.

The coexistence of two mesophases was observed in the mixtures at the temperature where the liquid crystal solvents are nematic. In addition, it was possible to detect organized microstructures consisting of the liquid crystalline polymer in the smectic phase, suspended in the isotropic matrix of the solvent.

Finally, when DSC and even POM fail, SAXS remains an important tool to determine the liquid crystal phase behaviour of complex systems such as those studied here.

The authors wish to acknowledge CNPq/Brazil and CAPES/COFECUB for financial support, and the staff of the BM2 beamline at the ESRF (France) and D11A beamline at the LNLS (Brazil). Dr Paulo Gonçalves is acknowledged for theoretical calculations.

References

[1] McCormick, D. T., Chavers, R., and Guymon, A., 2001, *Macromolecules*, **34,** 6929.

[2] Guymon, C. A., Hoggan, E. N., Clark, N. A., and Bowman, C. N., 1997, *Science*, **275,** 57.

[3] Drzaic, P. S., 1995, *Liquid Crystal Dispersions* (Singapore: World Scientific).

[4] Crawford, G. P., and Zumer, S., 1996, *Liquid Crystals in Complex Geometries* (London: Taylor and Francis).

[5] Corvazier, L., and Zhao, Y., 1999, *Macromolecules*, **32,** 3195.

[6] Kyu, T., and Chiu, H.-W., 1996, *Phys. Rev. E*, **53,** 3618.

[7] Matsuyama, A., and Kato, T., 1999, *Phys. Rev. E*, **59,** 763.

[8] Caerels, J., Glorieux, C., and Thoen, J., 2002, *Phys. Rev. E*, **65,** 1.

[9] Nwabunna, D., and Kyu, T., 1999, *Macromolecules*, **32,** 664.

[10] Kyu, T., and Chiu, H.-W., 1997, *Phys. Rev. E*, **55,** 7105.

[11] Roussel, F., and Buisine, J.-M., 2000, *Phys. Rev. E*, **62,** 2310.

[12] Fung, I. K., Borstnik, A., Žumer, S., Yang, D. K., and Doane, J. W., 1997, *Phys. Rev. E*, **55,** 1637.

[13] Liu, P. Y., Jamieson, A., and Ning, Y., 2000, *Macromolecules*, **33,** 1692.

[14] Merlo, A. A., Magnago, R. V., Vollmer, A. F., Mauller, R. S., Pereira, F. V., and da Silveira, N. P., 1999, *Polym. Bull.*, **42,** 551.

[15] Merlo, A. A., Ritter, O. M., Pereira, F. V., and da Silveira, N. P., 2001, *J. Braz. Chem. Soc.*, **12,** 184.

[16] Ritter, O. M. S., Merlo, A. A., Pereira, F. V., da Silveira, N. P., Geissler, E., and Schpector, J. Z., 2002, *Liq. Cryst.*, **29,** 1187.

[17] Pereira, F. V., Merlo, A. A., and da Silveira, N. P., 2002, *Polymer*, **43,** 3901.

[18] Stewart, J. J. P., 1989, *J. comput. Chem.*, **10,** 209.

[19] Pascual-Ahuir, J. L., and Silla, E., 1990, *J. Comput. Chem.*, **11,** 1047.

[20] Silla, E., Tunon, I., and Pascual-Ahuir, J. L., 1991, *J. Comput. Chem.*, **12,** 1077.

[21] Davidson, P., 1996, *Prog. polym. Sci.*, **21,** 893.

[22] Flory, P. J., 1953, *Principles of Polymer Chemistry* (Ithaca: Cornell University Press).

[23] McMillan, W. L., 1971, *Phys. Rev. A.*, **4,** 1238.